

Averaged resonant equations for non-gravitational effects without a spherical symmetry and their application for an interstellar gas flow

P. Pástor

Tekov Observatory, Sokolovská 21, 934 01 Levice, Slovak Republic

pavol.pastor@hvezdarenlevice.sk, pastor.pavol@gmail.com

ABSTRACT

Within the framework of the circular restricted three body problem we investigate the motion of a dust particle captured into a mean motion resonance with a planet under the action of non-gravitational effects. From equations of motion in a near-canonical form averaged resonant equations are derived. The averaged resonant equations describe secular variations of the particle orbit in the mean motion resonance. The secular variations of the particle orbit caused by the non-gravitational effects can depend on the orientation of the orbit in space. The averaged resonant equations are derived with this dependence taken into account. We also present an alternative way how the averaged resonant equations can be derived. We applied derived theory for the case when non-gravitational effects are the Poynting-Robertson effect, radial stellar wind and interstellar wind. Obtained analytical and numerical results are in excellent agreement in the Solar system. We found that types of orbits correspond to libration centers of conservative problem. We show that for the considered non-gravitational effects from the averaged resonant equations any stationary solution can not be obtained.

1. Introduction

A small body orbiting a star with a planet is affected by the planet's gravity field. When orbital periods of the body and the planet are in a ratio of small natural numbers mean motion resonances (MMRs) can occur. If the body is captured in an MMR, then changes of the semimajor axis are balanced by resonant interaction with the planet's gravity field. Examples of MMRs in the Solar system are numerous. We can mention MMRs of asteroids with Jupiter which result in formation of the Kirkwood gaps in the main asteroid belt (Kirkwood 1867), MMRs of particles in the Saturn's rings with his moons, MMRs of Edgeworth-Kuiper belt objects with Neptune, MMRs of dust particles with the Earth (Brownlee 1994; Dermott et al. 1994; Reach et al. 1995) and so on. Since the observational confirmation of the dust particles captured in MMRs with the Earth by satellites *IRAS* (Dermott et al. 1994) and *COBE* (Reach et al. 1995), unknown properties of orbital evolutions for dust particles captured in MMRs became an interesting topic of research. If the planet moves in a circular orbit around the star and the mass of the particle

is negligible in comparison with the mass of the star and also in comparison with the mass of the planet, we have a special gravitational problem of three bodies. This gravitational problem is called the circular restricted three-body problem (CR3BP) in celestial mechanics. Unlike asteroids, the dust particles can be significantly affected by the electromagnetic radiation and the stellar wind. The particle acceleration caused by the electromagnetic radiation described by Poynting-Robertson (PR) effect (Poynting 1904; Robertson 1937; Klačka 2008; Klačka et al. 2013) was used within the framework of the planar CR3BP by Beaugé & Ferraz-Mello (1994) in order to obtain stationary solutions for the dust particles captured in MMRs. They found that for all dust particles captured in a given exterior resonance (the particle orbital period in the exterior resonance is larger than the planet orbital period) eccentricities of orbits approach to a constant value which they called “universal eccentricity”. Their derivation starts from a near-canonical form of equations of motion in cartesian coordinates with the PR effect used as a dissipative external acceleration. The “universal eccentricity” was confirmed using a different derivation starting from the secular time derivative of the Tisserand parameter by Liou & Zook (1997). In Liou & Zook (1997) also a general relation between secular time derivatives of eccentricity and inclination during the orbital evolution of the dust particle captured in an MMR in the CR3BP with the PR effect and radial stellar wind (Gustafson 1994; Klačka et al. 2012) was found. Influence of the PR effect and non-radial stellar wind (Klačka et al. 2012) on the secular evolution of eccentricity for the dust particle captured in an MMR within the framework of the planar CR3BP was analytically investigated in Klačka et al. (2008) and Pástor et al. (2009). The secular evolutions of orbital eccentricity and argument of perihelion of the dust particle captured in an MMR in the planar circular and elliptical restricted three-body problem with the PR effect were numerically investigated in Pástor, Klačka & Kómar (2009). The PR effect and stellar wind are not the only non-gravitational effects which can affect the orbital motion of dust particles. Influence of an interstellar wind on the motion of the dust particles was already mentioned in Whipple (1955). Observations of debris disks around stars show that the interaction of the interstellar wind with the disk dust particles can change the shape of the debris disks (Hines et al. 2007; Maness et al. 2009; Debes, Weinberger & Kuchner 2009; Buenzli et al. 2010; Rodigas et al. 2012). From only 16 debris disks resolved in scattered light (Golimowski et al. 2011) as much as 3 disks show a changed morphology caused by the interaction with surrounding interstellar matter. The acceleration acting on a spherical body moving through an interstellar gas was published in Baines, Williams & Asebiomo (1965). This acceleration was used in calculation of the secular time derivatives of all Keplerian orbital elements caused by an interstellar gas flow (IGF) for arbitrary orientation of the orbit in Pástor, Klačka & Kómar (2011) and Pástor (2012b). The secular decrease of the semimajor axis for all initial conditions was found. This result was confirmed analytically by Belyaev & Rafikov (2010) (preprint of Pástor, Klačka & Kómar 2011 was cited in Belyaev & Rafikov 2010) and numerically by Marzari & Thébault (2011) and Marzari (2012). Belyaev & Rafikov (2010) used an orbit-averaged Hamiltonian approach to solve for the orbital evolution of a dust particle in a Keplerian potential subject to an additional constant force. If the speed of the IGF is much greater than the speed of the dust grain in the stationary frame associated with the central object and also much greater than the mean thermal speed of the gas

in the flow, then the acceleration caused by the IGF reduces into a constant vector. Therefore, the problem which they solved can be applied for the orbital motion of the dust particle under the action of an IGF. The secular orbital motion in this case can be completely solved analytically (Pástor 2012a). In Pástor (2013) the method used in Liou & Zook (1997) for the PR effect and radial stellar wind was generalized for arbitrary non-gravitational effects with known secular time derivatives of orbital elements. In (Pástor 2013) also results of Pástor (2012b) were used in order to obtain the secular time derivative of orbit eccentricity for the dust particle captured in an MMR within the framework of the planar CR3BP with the PR effect, radial stellar wind and IGF. The agreement between analytical and numerical results in Pástor (2013) was excellent for the IGF in the Solar system. Results show that two sets of orbital evolutions divided by a strong boundary in initial conditions exist for the exterior 2/1 resonance. Also some kind of stabilization was found in one of these sets. These results motivated us to determine some basic properties of the orbital evolution of the dust particle captured in an MMR in the planar CR3BP with the PR effect, radial stellar wind and IGF using improved methods from Beaugé & Ferraz-Mello (1993).

2. Averaged resonant equations

We will consider the motion of a homogeneous spherical dust particle in the vicinity of a star with one planet moving in a circular orbit. The gravitational problem is called the circular restricted three-body problem in celestial mechanics. Into the framework of the CR3BP we add also non-gravitational effects. The secular variations of the particle orbit caused by the non-gravitational effects can depend on the orientation of the orbit in space. Taking into account this dependence we improve method presented in Beaugé & Ferraz-Mello (1993) for study of problems which involve non-gravitational effects without a rotational symmetry around an axis going through the star.

Equation of motion can be written in the following form

$$\frac{d\vec{v}}{dt} = \frac{\partial F}{\partial \vec{r}} + \vec{Y} , \quad (1)$$

where $\vec{v} = d\vec{r}/dt$ is the velocity of the dust particle, \vec{r} is the position vector of the dust particle with respect to the star, F is the Hamiltonian of the conservative system and \vec{Y} is the non-conservative part of the acceleration. If we add to Eq. (1) equations for the velocity in the cartesian coordinates we obtain a system of equations in the near-canonical form

$$\frac{d\vec{r}}{dt} = -\frac{\partial F}{\partial \vec{v}} , \quad \frac{d\vec{v}}{dt} = \frac{\partial F}{\partial \vec{r}} + \vec{Y} . \quad (2)$$

Following Beaugé & Ferraz-Mello (1993) we use canonical variables derived from the Delaunay variables in the extended phase space. The canonical variables are $l_j = (\lambda, \tilde{\omega}, t)$ and $L_j = (L, G - L, \Lambda)$, where λ is the mean longitude, $\tilde{\omega}$ is the longitude of pericentre, $L = \sqrt{\mu(1 - \beta)}a$, $G = L\sqrt{1 - e^2}$ and Λ is the canonical momentum conjugated to the time. In the canonical variables $\mu = G_0 M_\star$, G_0 is the gravitational constant, M_\star is the mass of the star, a is the semimajor axis of

the particle orbit and e is the eccentricity of the particle orbit. From the non-gravitational effects, the electromagnetic radiation of the star in the form of the Poynting-Robertson (PR) effect is most often considered. The parameter β is defined as the ratio of the electromagnetic radiation pressure force and the gravitational force between the star and the particle at rest with respect to the star

$$\beta = \frac{3L_\star \bar{Q}'_{\text{pr}}}{16\pi c \mu R \varrho} . \quad (3)$$

Here, L_\star is the stellar luminosity, \bar{Q}'_{pr} is the dimensionless efficiency factor for radiation pressure averaged over the stellar spectrum and calculated for the radial direction ($\bar{Q}'_{\text{pr}} = 1$ for a perfectly absorbing sphere) and R is the radius of the dust particle with the mass density ϱ . The radial term not depending on the particle velocity in the PR effect (Eq. 21) can be added to the stellar gravity because its net effect is only to reduce the mass of the star to $M_\star(1 - \beta)$. Therefore, we use $L = \sqrt{\mu(1 - \beta)a}$. Using the Brouwer-Hori theorem (Brouwer & Hori 1961) we can transform Eqs. (2) into a new system of near-canonical equations

$$\frac{dl_j}{dt} = -\frac{\partial F}{\partial L_j} + Q_j , \quad \frac{dL_j}{dt} = \frac{\partial F}{\partial l_j} + P_j , \quad (4)$$

where

$$Q_j = \sum_{k=1}^3 Y_k \frac{\partial r_k}{\partial L_j} , \quad P_j = \sum_{k=1}^3 Y_k \frac{\partial r_k}{\partial l_j} \quad (5)$$

and r_k are the cartesian coordinates of the particle position vector with respect to the star. Cumbersome calculation of the partial derivatives finally yields

$$\begin{aligned} Q_1 &= \frac{2}{L} \vec{Y} \cdot \vec{r} + (1 - \alpha) Q_2 , \\ Q_2 &= \frac{a}{Le} \vec{Y} \begin{pmatrix} \alpha \cos \tilde{\omega} - e \sin E \sin \tilde{\omega} \\ \alpha \sin \tilde{\omega} + e \sin E \cos \tilde{\omega} \end{pmatrix} - \frac{\alpha}{Le} P_1 \sin E , \\ P_1 &= \frac{1}{n} \vec{Y} \cdot \vec{v} , \\ P_2 &= \vec{Y} \begin{pmatrix} -r_2 \\ r_1 \end{pmatrix} - P_1 , \end{aligned} \quad (6)$$

where $\alpha = \sqrt{1 - e^2}$, E is the eccentric anomaly and $n = \sqrt{\mu(1 - \beta)/a^3}$ is the mean motion of the particle. Eqs. (6) differ from equations in Beaugé & Ferraz-Mello (1993) due to the dependence of the partial derivatives on the orientation of the particle orbit in space which is considered. The Hamiltonian of the conservative system in the new variables is

$$F = \frac{\mu^2(1 - \beta)^2}{2L^2} - \Lambda + R , \quad (7)$$

where R is the disturbing function

$$R = G_0 M_{\text{P}} \left(\frac{1}{|\vec{r} - \vec{r}_{\text{P}}|} - \frac{\vec{r} \cdot \vec{r}_{\text{P}}}{r_{\text{P}}^3} \right) , \quad (8)$$

M_P is the mass of the planet and \vec{r}_P is the position vector of the planet with respect to the star. The subscript P will be used for quantities belonging to the planet. In order to investigate behavior of the particle captured in an MMR with the planet in a circular orbit we will use the canonical resonant variables $H, K, \sigma_1, J_1, \sigma_2, J_2$

$$\begin{aligned} H &= \sqrt{2|L - G|} \sin(\psi/q - \tilde{\omega}) , & K &= \sqrt{2|L - G|} \cos(\psi/q - \tilde{\omega}) , \\ \sigma_1 &= \psi/q - \tilde{\omega}_P , & J_1 &= G + \Lambda/n_P , \\ \sigma_2 &= (\lambda - \lambda_P)/q , & J_2 &= (p + q)L + p\Lambda/n_P , \end{aligned} \quad (9)$$

where $\psi = (p + q)\lambda_P - p\lambda$. The second application of the Brouwer-Hori theorem yields equations which are formally consistent with the set of equation presented in Beaugé & Ferraz-Mello (1993)

$$\begin{aligned} \frac{dH}{dt} &= -\frac{\partial F}{\partial K} - \frac{H}{H^2 + K^2} P_2 + K(sQ_1 + Q_2) , \\ \frac{dK}{dt} &= \frac{\partial F}{\partial H} - \frac{K}{H^2 + K^2} P_2 - H(sQ_1 + Q_2) , \\ \frac{d\sigma_1}{dt} &= -\frac{\partial F}{\partial J_1} + sQ_1 , \\ \frac{dJ_1}{dt} &= \frac{\partial F}{\partial \sigma_1} + P_1 + P_2 , \\ \frac{d\sigma_2}{dt} &= -\frac{\partial F}{\partial J_2} - \frac{1}{q} Q_1 , \\ \frac{dJ_2}{dt} &= \frac{\partial F}{\partial \sigma_2} + (p + q)P_1 , \end{aligned} \quad (10)$$

where $s = p/q$. All terms in the disturbing function depended on $\tilde{\omega}_P$ must be multiplied by a power of e_1 due to the d'Alembert property (Murray & Dermott 1999). Because we are considering only the circular planetary orbits and $\tilde{\omega}_P$ is only present in σ_1 , we have $\partial F/\partial \sigma_1 = 0$. Eqs. (10) have to be averaged over a synodic period. The change of σ_2 is equal to 2π during the synodic period. Over the synodic period averaged term $\partial F/\partial \sigma_2$ in Eqs. (10) is $1/2\pi \int_0^{2\pi} \partial F/\partial \sigma_2 d\sigma_2 = F(2\pi) - F(0) = 0$ due to a periodicity of the disturbing function with this period (during averaging). Thus, Eqs. (10) averaged over the synodic period are

$$\begin{aligned} \frac{dH}{dt} &= -\frac{\partial F}{\partial K} - \frac{H}{H^2 + K^2} \langle P_2 \rangle + K(s \langle Q_1 \rangle + \langle Q_2 \rangle) , \\ \frac{dK}{dt} &= \frac{\partial F}{\partial H} - \frac{K}{H^2 + K^2} \langle P_2 \rangle - H(s \langle Q_1 \rangle + \langle Q_2 \rangle) , \\ \frac{d\sigma_1}{dt} &= -\frac{\partial F}{\partial J_1} + s \langle Q_1 \rangle , \\ \frac{dJ_1}{dt} &= \langle P_1 \rangle + \langle P_2 \rangle , \\ \frac{d\sigma_2}{dt} &= -\frac{\partial F}{\partial J_2} - \frac{1}{q} \langle Q_1 \rangle , \\ \frac{dJ_2}{dt} &= (p + q) \langle P_1 \rangle . \end{aligned} \quad (11)$$

In resonant problems is convenient to study behavior in the non-canonical variables $(k, h) = (e \cos \sigma_0, e \sin \sigma_0)$, where $\sigma_0 = \psi/q - \tilde{\omega}$. J_1 can be expressed using L, J_2, k and h in the disturbing function R . The number of equations can be reduced from six to five because dJ_2/dt can be expressed using dL/dt and dJ_1/dt . Equation for dJ_1/dt can be replaced with equation for dL/dt . Further reduction of the number of equations is possible because σ_2 is cyclic and can be ignored. Therefore only four equations remain and the equations are

$$\begin{aligned} \frac{dk}{dt} &= \frac{\alpha}{L} \frac{\partial R}{\partial h} - h \frac{d\sigma_1}{dt} - \frac{k\alpha}{L(1+\alpha)} \frac{dL}{dt} - \frac{k\alpha}{Le^2} \langle P_2 \rangle - h \langle Q_2 \rangle , \\ \frac{dh}{dt} &= -\frac{\alpha}{L} \frac{\partial R}{\partial k} + k \frac{d\sigma_1}{dt} - \frac{h\alpha}{L(1+\alpha)} \frac{dL}{dt} - \frac{h\alpha}{Le^2} \langle P_2 \rangle + k \langle Q_2 \rangle , \\ \frac{dL}{dt} &= s \left(h \frac{\partial R}{\partial k} - k \frac{\partial R}{\partial h} \right) + \langle P_1 \rangle , \\ \frac{d\sigma_1}{dt} &= n_P \frac{p+q}{q} - ns + \frac{2sL}{\mu(1-\beta)} \frac{\partial R}{\partial a} - \frac{\alpha s}{L(1+\alpha)} \left(k \frac{\partial R}{\partial k} + h \frac{\partial R}{\partial h} \right) + s \langle Q_1 \rangle . \end{aligned} \quad (12)$$

Eqs. (12) represent averaged resonant equations with included the directional character of non-conservative acceleration \vec{Y} . It is worth mentioning that the averaged values of the non-conservative terms $\langle Q_j \rangle$ and $\langle P_j \rangle$ can be expressed using averaged values of $da/dt, de/dt, d\tilde{\omega}/dt$ and $d\sigma_b/dt + t dn/dt$ caused by the non-gravitational effects only. The angle σ_b is defined so that the mean anomaly can be computed from $M = nt + \sigma_b$ (Bate, Mueller & White 1971). We can use on the left-hand sides of Eqs. (12) the Lagrange's planetary equations in the following form

$$\begin{aligned} \frac{da}{dt} &= \frac{2}{na} \frac{\partial R}{\partial \sigma_b} + \left\langle \frac{da}{dt} \right\rangle_{\text{EF}} , \\ \frac{de}{dt} &= \frac{\alpha^2}{na^2e} \frac{\partial R}{\partial \sigma_b} - \frac{\alpha}{na^2e} \frac{\partial R}{\partial \tilde{\omega}} + \left\langle \frac{de}{dt} \right\rangle_{\text{EF}} , \\ \frac{d\sigma_b}{dt} + t \frac{dn}{dt} &= -\frac{2}{na} \frac{\partial R}{\partial a} - \frac{\alpha^2}{na^2e} \frac{\partial R}{\partial e} + \left\langle \frac{d\sigma_b}{dt} + t \frac{dn}{dt} \right\rangle_{\text{EF}} , \\ \frac{d\tilde{\omega}}{dt} &= \frac{\alpha}{na^2e} \frac{\partial R}{\partial e} + \left\langle \frac{d\tilde{\omega}}{dt} \right\rangle_{\text{EF}} . \end{aligned} \quad (13)$$

$\partial R/\partial a$ in Eqs. (13) is calculated in such a way that n is treated as a constant (Danby 1988). For this particular case this is the only correct way and this also cancels term $\langle t dn/dt \rangle_G$ (where the subscript G denotes that the change is caused by the gravitation only) in the derivation resulting from $d\sigma_1/dt$ in Eqs. (12). During these operations the following relations must be used

$$\begin{aligned} \frac{\partial R}{\partial \sigma_b} &= -s \frac{\partial R}{\partial \sigma_0} , \\ \frac{\partial R}{\partial \tilde{\omega}} &= -\frac{p+q}{q} \frac{\partial R}{\partial \sigma_0} , \\ \frac{\partial R}{\partial \sigma_0} &= k \frac{\partial R}{\partial h} - h \frac{\partial R}{\partial k} , \\ e \frac{\partial R}{\partial e} &= k \frac{\partial R}{\partial k} + h \frac{\partial R}{\partial h} . \end{aligned} \quad (14)$$

The obtained relations are

$$\begin{aligned}
\langle Q_1 \rangle &= - \left\langle \frac{d\tilde{\omega}}{dt} \right\rangle_{\text{EF}} - \left\langle \frac{d\sigma_b}{dt} + t \frac{dn}{dt} \right\rangle_{\text{EF}} , \\
\langle Q_2 \rangle &= - \left\langle \frac{d\tilde{\omega}}{dt} \right\rangle_{\text{EF}} , \\
\langle P_1 \rangle &= \frac{na}{2} \left\langle \frac{da}{dt} \right\rangle_{\text{EF}} , \\
\langle P_2 \rangle &= - \frac{na(1-\alpha)}{2} \left\langle \frac{da}{dt} \right\rangle_{\text{EF}} - \frac{na^2e}{\alpha} \left\langle \frac{de}{dt} \right\rangle_{\text{EF}} .
\end{aligned} \tag{15}$$

Eqs. (15) hold for arbitrary non-gravitational effects.

3. Orbit eccentricity secular time derivative

The second equation of Eqs. (13) yields

$$\begin{aligned}
\frac{de}{dt} &= \frac{\alpha^2}{na^2e} \frac{\partial R}{\partial \sigma_b} - \frac{\alpha}{na^2e} \frac{\partial R}{\partial \tilde{\omega}} + \left\langle \frac{de}{dt} \right\rangle_{\text{EF}} \\
&= \frac{\alpha^2}{2ae} \left(\frac{da}{dt} - \left\langle \frac{da}{dt} \right\rangle_{\text{EF}} \right) + \frac{\alpha}{na^2e} \frac{p+q}{q} \frac{\partial R}{\partial \sigma_0} + \left\langle \frac{de}{dt} \right\rangle_{\text{EF}} ,
\end{aligned} \tag{16}$$

where also the first equation of Eqs. (13) and the second equation of Eqs. (14) were used. If we use the first equation of Eqs. (14) and the first equation of Eqs. (13) in Eq. (16), then we obtain

$$\begin{aligned}
\frac{de}{dt} &= \frac{\alpha^2}{2ae} \left(\frac{da}{dt} - \left\langle \frac{da}{dt} \right\rangle_{\text{EF}} \right) - \frac{\alpha}{2ae} \frac{p+q}{p} \left(\frac{da}{dt} - \left\langle \frac{da}{dt} \right\rangle_{\text{EF}} \right) + \left\langle \frac{de}{dt} \right\rangle_{\text{EF}} \\
&= \frac{\alpha}{2ae} \left(\alpha - \frac{p+q}{p} \right) \frac{da}{dt} + \frac{\alpha}{2ae} \left(\frac{p+q}{p} - \alpha \right) \left\langle \frac{da}{dt} \right\rangle_{\text{EF}} + \left\langle \frac{de}{dt} \right\rangle_{\text{EF}} .
\end{aligned} \tag{17}$$

This equation can be averaged over a resonant libration period of the semimajor axis and the result is

$$\left\langle \frac{de}{dt} \right\rangle = \frac{\alpha}{2ae} \left(\frac{p+q}{p} - \alpha \right) \left\langle \frac{da}{dt} \right\rangle_{\text{EF}} + \left\langle \frac{de}{dt} \right\rangle_{\text{EF}} , \tag{18}$$

because

$$\left\langle \frac{da}{dt} \right\rangle = 0 . \tag{19}$$

Eq. (18) is consistent with the same result obtained from averaging of the time derivative of Tisserand parameter over the resonant libration period of the semimajor axis (see Pástor 2013). We can rewrite Eq. (18) using the averaged non-conservative terms in Eqs. (15)

$$\left\langle \frac{de}{dt} \right\rangle = \frac{\alpha}{na^2e} \left(\frac{1}{s} \langle P_1 \rangle - \langle P_2 \rangle \right) . \tag{20}$$

4. Effects considered

We take into account the electromagnetic radiation of the star, radial stellar wind and interstellar gas flow (IGF).

4.1. Electromagnetic radiation

The acceleration of the homogeneous spherical dust particle caused by the electromagnetic radiation of the star is given by the PR effect (Poynting 1904; Robertson 1937; Klačka 2008; Klačka et al. 2013). The acceleration to the first order in v/c (v is the speed of the dust particle with respect to the star and c is the speed of light in vacuum) has the form

$$\frac{d\vec{v}}{dt} = \beta \frac{\mu}{r^2} \left[\left(1 - \frac{\vec{v} \cdot \vec{e}_R}{c} \right) \vec{e}_R - \frac{\vec{v}}{c} \right], \quad (21)$$

where $r = |\vec{r}|$ is the distance from the star, $\vec{e}_R = \vec{r}/r$ is the radial unit vector.

4.2. Radial stellar wind

Acceleration caused by the radial stellar wind to the first order of v/c and the first order of v/u (u is the speed of the stellar wind with respect to the star) is given by (Klačka et al. 2012, Eq. 37):

$$\frac{d\vec{v}}{dt} = \frac{\eta}{Q'_{\text{pr}}} \beta \frac{u}{c} \frac{\mu}{r^2} \left[\left(1 - \frac{\vec{v} \cdot \vec{e}_R}{u} \right) \vec{e}_R - \frac{\vec{v}}{u} \right]. \quad (22)$$

η is the ratio of stellar wind energy to electromagnetic stellar energy, both radiated per unit of time

$$\eta = \frac{4\pi r^2 u}{L_\star} \sum_{i=1}^N n_{\text{sw } i} m_{\text{sw } i} c^2, \quad (23)$$

where $m_{\text{sw } i}$ and $n_{\text{sw } i}$, $i = 1$ to N , are the masses and concentrations of the stellar wind particles at a distance r from the star ($u = 450$ km/s and $\eta = 0.38$ for the Sun, Klačka et al. 2012).

4.3. Interstellar gas flow

The acceleration caused by the flow of neutral gas can be given in the form (Baines, Williams & Asebiomo 1965)

$$\frac{d\vec{v}}{dt} = - \sum_i c_{\text{Di}} \gamma_i |\vec{v} - \vec{v}_F| (\vec{v} - \vec{v}_F). \quad (24)$$

The sum in Eq. (24) runs over all particle species i . \vec{v}_F is the velocity of the IGF in the frame associated with the star, c_{Di} is the drag coefficient, and γ_i is the collision parameter. The drag

coefficient can be calculated from

$$c_{\text{Di}}(s_i) = \frac{1}{\sqrt{\pi}} \left(\frac{1}{s_i} + \frac{1}{2s_i^3} \right) e^{-s_i^2} + \left(1 + \frac{1}{s_i^2} - \frac{1}{4s_i^4} \right) \text{erf}(s_i) + (1 - \delta_i) \left(\frac{T_d}{T_i} \right)^{1/2} \frac{\sqrt{\pi}}{3s_i}, \quad (25)$$

where $\text{erf}(s_i)$ is the error function $\text{erf}(s_i) = 2/\sqrt{\pi} \int_0^{s_i} e^{-t^2} dt$, δ_i is the fraction of impinging particles specularly reflected at the surface (for the resting particles, there is assumed diffuse reflection) (Baines, Williams & Asebiomo 1965; Gustafson 1994), T_d is the temperature of the dust grain, and T_i is the temperature of the i th gas component. s_i is defined as a molecular speed ratio

$$s_i = \sqrt{\frac{m_i}{2kT_i}} U. \quad (26)$$

Here, m_i is the mass of the neutral atom in the i th gas component, k is Boltzmann's constant, and $U = |\vec{v} - \vec{v}_F|$ is the relative speed of the dust particle with respect to the gas. For the collision parameter, we can write

$$\gamma_i = n_i \frac{m_i}{m} A, \quad (27)$$

where n_i is the concentration of the interstellar neutral atoms of type i , and $A = \pi R^2$ is the geometrical cross section of the spherical dust grain and m is the grain mass. Using the approximation that the speed of the IGF is much greater than the speed of the dust grain in the frame associated with the star ($|\vec{v}| = v \ll |\vec{v}_F| = v_F$) we can approximate the expression for the relative speed

$$U = |\vec{v} - \vec{v}_F| = \sqrt{v^2 + v_F^2 - 2\vec{v} \cdot \vec{v}_F} \approx v_F \left(1 - \frac{\vec{v} \cdot \vec{v}_F}{v_F^2} \right). \quad (28)$$

The same approximation can be used also in Eq. (25). The result is

$$\begin{aligned} c_{\text{Di}}(s_i) &\approx c_{\text{Di}}(s_{0i}) + \left(\frac{dc_{\text{Di}}}{ds_i} \right)_{s_i=s_{0i}} (s_i - s_{0i}) \\ &\equiv c_{\text{Di}}(s_{0i}) + \left(\frac{dc_{\text{Di}}}{ds_i} \right)_{s_i=s_{0i}} \sqrt{\frac{m_i}{2kT_i}} (U - v_F) \\ &\approx c_{0i} - k_i \frac{\vec{v} \cdot \vec{v}_F}{v_F}, \end{aligned} \quad (29)$$

where

$$\begin{aligned} s_{0i} &\equiv \sqrt{\frac{m_i}{2kT_i}} v_F, \\ c_{0i} &\equiv c_{\text{Di}}(s_{0i}), \\ k_i &\equiv \left(\frac{dc_{\text{Di}}}{ds_i} \right)_{s_i=s_{0i}} \sqrt{\frac{m_i}{2kT_i}}. \end{aligned} \quad (30)$$

We can rewrite Eq. (24) using Eqs. (28) and (29) into the following form

$$\frac{d\vec{v}}{dt} = - \sum_i c_{0i} \gamma_i v_F^2 \left[\frac{\vec{v}}{v_F} - \frac{\vec{v}_F}{v_F} + g_i \frac{\vec{v} \cdot \vec{v}_F}{v_F^2} \frac{\vec{v}_F}{v_F} \right], \quad (31)$$

where

$$g_i = 1 + \frac{k_i}{c_{0i}} v_F = \frac{1}{c_{0i}} \left[\frac{1}{\sqrt{\pi}} \left(\frac{1}{s_{0i}} - \frac{3}{2s_{0i}^3} \right) e^{-s_{0i}^2} + \left(1 - \frac{1}{s_{0i}^2} + \frac{3}{4s_{0i}^4} \right) \text{erf}(s_{0i}) \right]. \quad (32)$$

Eq. (31) was already used in Pástor (2012b) for derivation of secular time derivatives of the Keplerian orbital elements caused by the IGF.

5. Equation of motion

Since we want to study the motion of dust particle in a frame of reference associated with the star in the planar CR3BP, we must add to the sum of Eqs. (21), (22) and (24) the corresponding gravitational accelerations. If we assume that $(\eta/\bar{Q}'_{\text{pr}})(u/c) \ll 1$, the particle equation of motion has the following form

$$\begin{aligned} \frac{d\vec{v}}{dt} = & -\frac{\mu}{r^2} (1 - \beta) \vec{e}_R - \frac{G_0 M_{\text{P}}}{|\vec{r} - \vec{r}_{\text{P}}|^3} (\vec{r} - \vec{r}_{\text{P}}) - \frac{G_0 M_{\text{P}}}{r_{\text{P}}^3} \vec{r}_{\text{P}} \\ & - \beta \frac{\mu}{r^2} \left(1 + \frac{\eta}{\bar{Q}'_{\text{pr}}} \right) \left(\frac{\vec{v} \cdot \vec{e}_R}{c} \vec{e}_R + \frac{\vec{v}}{c} \right) \\ & - \sum_i c_{\text{Di}} \gamma_i |\vec{v} - \vec{v}_{\text{F}}| (\vec{v} - \vec{v}_{\text{F}}), \end{aligned} \quad (33)$$

where $r_{\text{P}} = |\vec{r}_{\text{P}}|$. Eq. (33) can be numerically solved in order to obtain the motion of the dust particle.

6. Averaged resonant equations for the considered non-gravitational effects

Because we assume that the electromagnetic radiation and radial stellar wind are independent on the direction from the star (spherical symmetry), secular variations of any given particle orbit are independent of the orbit orientation in space for the accelerations caused by the PR effect and radial stellar wind. Therefore, for the PR effect and radial stellar wind the theory presented in Beaugé & Ferraz-Mello (1993) can be used. However, secular variations of the particle orbit for the acceleration caused by the IGF depend on the orientation of the orbit with respect to the IGF velocity vector and in this case the theory developed in Sec. 2 must be used. The last term in Eq. (33) does not allow to determine directly the secular variations of the particle orbit caused by the IGF. Hence, in analytical calculations we will use Eq. (31) instead of Eq. (24). Thus, the non-conservative part of the acceleration in Eq. (1) is

$$\begin{aligned} \vec{Y} = & -\beta \frac{\mu}{r^2} \left(1 + \frac{\eta}{\bar{Q}'_{\text{pr}}} \right) \left(\frac{\vec{v} \cdot \vec{e}_R}{c} \vec{e}_R + \frac{\vec{v}}{c} \right) \\ & - \sum_i c_{0i} \gamma_i v_{\text{F}}^2 \left[\frac{\vec{v}}{v_{\text{F}}} - \frac{\vec{v}_{\text{F}}}{v_{\text{F}}} + g_i \frac{\vec{v} \cdot \vec{v}_{\text{F}}}{v_{\text{F}}^2} \frac{\vec{v}_{\text{F}}}{v_{\text{F}}} \right]. \end{aligned} \quad (34)$$

We calculated average values of Q_i and P_i in Eqs. (6) using an assumption that properties of the IGF are constant. Results for the averaged non-conservative terms in Eqs. (12) are

$$\begin{aligned}
\langle Q_1 \rangle &= - \sum_i \frac{3c_{0i}\gamma_i v_{F_i} a e S}{L} + (1 - \alpha) \langle Q_2 \rangle , \\
\langle Q_2 \rangle &= \sum_i \frac{c_{0i}\gamma_i v_{F_i} a \alpha S}{2L} \left\{ \frac{3}{e} - \frac{\sigma g_i I}{v_F} \left[\frac{2\alpha^2}{(1 + \alpha)^2} - 1 \right] \right\} , \\
\langle P_1 \rangle &= - \frac{\beta \mu n}{2c\alpha^3} \left(1 + \frac{\eta}{\bar{Q}'_{\text{pr}}} \right) (3e^2 + 2) - \sum_i c_{0i}\gamma_i v_{F_i}^2 \sigma a \alpha \left[1 + \frac{g_i (S^2 + \alpha I^2)}{v_F^2 (1 + \alpha)} \right] , \\
\langle P_2 \rangle &= - \langle P_1 \rangle - \frac{\beta \mu n}{c} \left(1 + \frac{\eta}{\bar{Q}'_{\text{pr}}} \right) - \sum_i c_{0i}\gamma_i v_{F_i}^2 a \left[\frac{3eI}{2v_F} + \sigma \alpha^2 \left(1 + \frac{g_i}{2} \right) \right] , \tag{35}
\end{aligned}$$

where

$$\sigma = \frac{1}{v_F} \sqrt{\frac{\mu(1 - \beta)}{a(1 - e^2)}} , \tag{36}$$

$$\begin{aligned}
S &= v_{F1} \cos \tilde{\omega} + v_{F2} \sin \tilde{\omega} , \\
I &= -v_{F1} \sin \tilde{\omega} + v_{F2} \cos \tilde{\omega} , \tag{37}
\end{aligned}$$

with the cartesian coordinates of the interstellar gas flow velocity vector denoted as v_{Fk} . The equivalent way to obtain Eqs. (35) is to use the following identities in Eqs. (15)

$$\begin{aligned}
\left\langle \frac{da}{dt} \right\rangle_{\text{EF}} &= - \frac{\beta \mu}{ca\alpha^3} \left(1 + \frac{\eta}{\bar{Q}'_{\text{pr}}} \right) (2 + 3e^2) - \sum_i \frac{2c_{0i}\gamma_i v_{F_i}^2 \sigma a^2 \alpha}{L} \left[1 + \frac{g_i (S^2 + \alpha I^2)}{v_F^2 (1 + \alpha)} \right] , \\
\left\langle \frac{de}{dt} \right\rangle_{\text{EF}} &= - \frac{\beta \mu}{2ca^2 \alpha} \left(1 + \frac{\eta}{\bar{Q}'_{\text{pr}}} \right) 5e + \sum_i \frac{c_{0i}\gamma_i v_{F_i} a \alpha}{2L} \left[3I + \frac{\sigma g_i \alpha^2 (1 - \alpha) (I^2 - S^2)}{v_F e (1 + \alpha)} \right] , \\
\left\langle \frac{d\tilde{\omega}}{dt} \right\rangle_{\text{EF}} &= \sum_i \frac{c_{0i}\gamma_i v_{F_i} a \alpha S}{2L} \left\{ -\frac{3}{e} + \frac{\sigma g_i I}{v_F} \left[\frac{2\alpha^2}{(1 + \alpha)^2} - 1 \right] \right\} , \\
\left\langle \frac{d\sigma_b}{dt} + t \frac{dn}{dt} \right\rangle_{\text{EF}} &= \sum_i \frac{c_{0i}\gamma_i v_{F_i} a S}{2L} \left\{ \frac{3(1 + e^2)}{e} - \frac{\sigma g_i \alpha^2 I}{v_F} \left[\frac{2\alpha^2}{(1 + \alpha)^2} - 1 \right] \right\} . \tag{38}
\end{aligned}$$

The first three equations in Eqs. (38) were already obtained in Pástor (2012b) in slightly different equivalent form.

The time derivative of the orbit eccentricity averaged over the resonant libration period of the semimajor axis, obtained from Eq. (18) or Eq. (20), for the considered effects is

$$\begin{aligned}
\left\langle \frac{de}{dt} \right\rangle &= \frac{\beta \mu \alpha}{ca^2 e} \left(1 + \frac{\eta}{\bar{Q}'_{\text{pr}}} \right) \left(1 - \frac{2 + 3e^2}{2\alpha^3} \frac{p + q}{p} \right) \\
&+ \sum_i \frac{c_{0i}\gamma_i v_{F_i}^2 a \alpha}{L} \left\{ \frac{3}{2} \frac{I}{v_F} + \frac{\sigma \alpha^2}{e} \left(1 + \frac{g_i}{2} \right) - \frac{\sigma \alpha}{e} \left[1 + \frac{g_i (S^2 + \alpha I^2)}{v_F^2 (1 + \alpha)} \right] \frac{p + q}{p} \right\} . \tag{39}
\end{aligned}$$

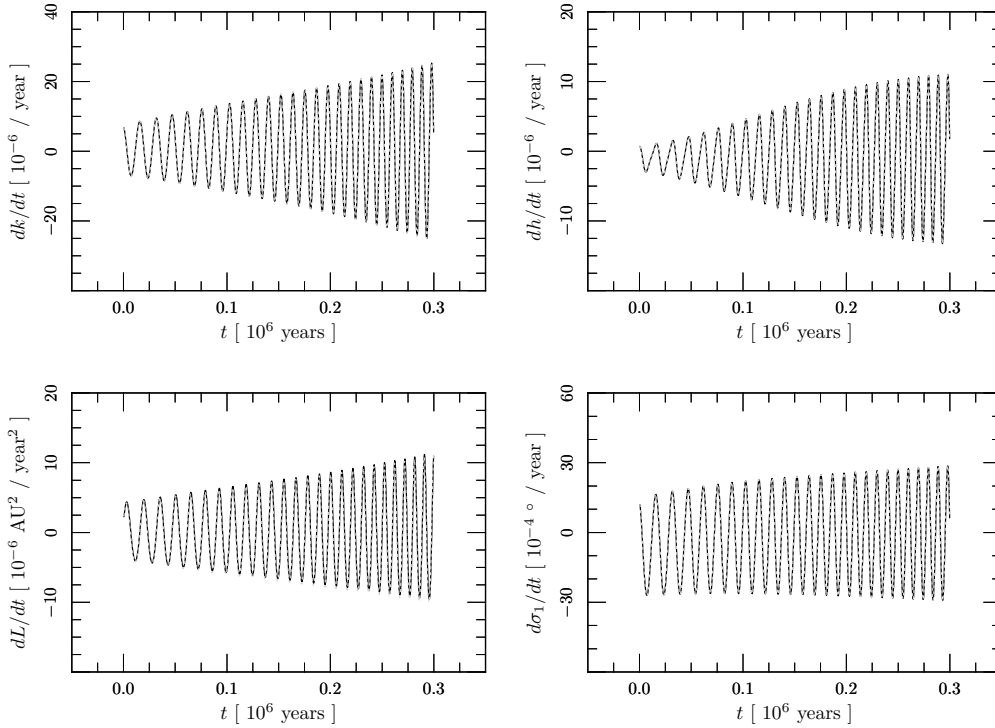


Fig. 1.— Comparison of over the synodic period averaged time derivatives of k , h , L and σ_1 obtained from a numerical solution of equation of motion (solid black line) and from the analytical theory (dashed gray line) for a dust particle with $R = 2 \mu\text{m}$, $\varrho = 1 \text{ g/cm}^3$, and $\bar{Q}'_{\text{pr}} = 1$ captured in an exterior mean motion orbital 2/1 resonance with Neptune under the action of the PR effect, radial solar wind and IGF.

7. Comparison of analytical and numerical results

Interstellar gas penetrates also into the heliosphere and can affect the motion of dust particles in the outer parts of the Solar system. The IGF in the Solar system arrives from direction $\lambda_{\text{ecl}} = 254.7^\circ$ (heliocentric ecliptic longitude) and $\beta_{\text{ecl}} = 5.2^\circ$ (heliocentric ecliptic latitude; Lallement et al. 2005). The IGF contains mainly hydrogen and helium atoms. Some of the atoms are ionized. The ionized hydrogen in the IGF can acquire electron from interstellar H° in the outer heliosheath during the passage into the heliopause (Frisch et al. 2009; Alouani-Bibi et al. 2011). Therefore, inside the heliopause are two populations of the neutral interstellar hydrogen. The primary population represent the original neutral hydrogen atoms of the IGF which penetrate into the heliopause. The secondary population is created by charge exchange in the outer heliosheath (between the bow shock and the heliopause). Neutral atoms from both the primary and the secondary population penetrate freely inside the heliopause. The solar wind density decreases as r^{-2} inside of the heliopause. Thus, the efficiency of charge exchange is reduced dramatically as compared with the efficiency in front of the heliopause, and the two populations flow through the inner heliosheath practically without

a change. We neglect influences of solar gravity and solar radiation pressure on the motion of neutral hydrogen inside the heliopause which is important only few AU from the Sun. For the same reason we neglect also losses of neutral hydrogen due to ionization by solar wind and solar extreme ultraviolet radiation inside the heliopause. Neutral interstellar helium flows freely through the outer heliosphere (with only $\leq 2\%$ filtration through charge exchange with H^+) and inside of the Earth’s orbit is ionized by photoionization and electron ionization (Frisch et al. 2009). We assumed that velocities and densities of both populations of the neutral hydrogen and the neutral helium can be approximated by constant values in the outer heliopause. The velocity vector of the IGF in the Solar system does not lie exactly in the Neptune orbital plane. The angle between direction of the interstellar gas velocity vector and the Neptune orbital plane is 3.7° . Obtained orbital evolutions of the dust particles under the action of the PR effect, radial solar wind and IGF are almost undistinguishable from coplanar case due to the small value of this angle (Pástor, Klačka & Kómar 2011). This can be understood using the secular time derivatives of orbital elements for arbitrary orientation of the orbit caused by the considered effects. The secular time derivatives are shown in Pástor (2012b). The secular time derivative of inclination caused by the PR effect and radial solar wind is zero and the secular time derivative of inclination caused by the IGF is proportional to the component of interstellar gas velocity vector normal to the particle orbital plane (approximately the orbital plane of Neptune in our case). Because the normal component of the interstellar gas velocity vector is small, the inclination of orbit can be approximated by a constant value (a value close to zero in our case). The fact that the velocity vector of the IGF does not lie exactly in the orbital plane of Neptune has also a positive effect. The IGF velocity and density are not significantly affected by the Sun because large part of the Neptune orbital plane is not in the “shadow” cast by the Sun in the IGF. The “shadow” goes beneath the Neptune orbital plane. We adopted the following densities and temperatures for various components in the IGF. $n_1 = 0.059 \text{ cm}^{-3}$ and $T_1 = 6100 \text{ K}$ for the primary population of neutral hydrogen (Frisch et al. 2009), $n_2 = 0.059 \text{ cm}^{-3}$ and $T_2 = 16500 \text{ K}$ for the secondary population of neutral hydrogen (Frisch et al. 2009) and finally $n_3 = 0.015 \text{ cm}^{-3}$ and $T_3 = 6300 \text{ K}$ for the neutral helium (Lallement et al. 2005). The assumed interstellar gas speed is equal for all components and identical to the speed of the neutral helium entering the Solar system $v_F = 26.3 \text{ km s}^{-1}$ (Lallement et al. 2005). The IGF velocity vector was rotated into the orbital plane of Neptune around an axis lying in the orbital plane of Neptune and perpendicular to the interstellar gas velocity vector in order to ensure the planar case in our numerical investigations.

For comparison of analytical and numerical results we used a dust particle with $R = 2 \mu\text{m}$, $\rho = 1 \text{ g/cm}^3$, and $\bar{Q}'_{\text{pr}} = 1$. We neglected the Lorentz force which is only important for submicrometer particles (Dohnanyi 1978; Leinert & Grün 1990; Dermott et al. 2001). Interval between collisions is of order 10^7 years for the particle with $R = 2 \mu\text{m}$ beyond the orbit of Neptune (Pástor, Klačka & Kómar 2011). We assumed that the atoms are specularly reflected at the surface of the dust grain ($\delta_i = 1$ in Eq. 25) and used an approximation that the drag coefficients are constant ($c_{D_i} = c_{D_i}(s_{0_i})$ and $g_i = 1$). The approximation that the drag coefficients are constant is usable if the inequality $|\vec{v}| \ll v_F$ holds during an orbit (for a comparison of evolutions see Fig. 5 in Pástor

Fig.	a_{in} [AU]	e_{in} [-]	$\tilde{\omega}_{\text{in}}$ [°]	f_{in} [°]
2	$a_{2/1} + 0.001$	0.6	295	0
3	$a_{2/1} + 0.001$	0.5	0	0
4	$a_{2/1} + 0.001$	0.5	90	0

Table 1: The initial conditions of the dust particle for the numerical solutions of equation of motion with results depicted in Figs. 2, 3 and 4.

2012b). Over the synodic period averaged time derivatives of parameters k , h , L and σ_1 obtained from a numerical solution of Eq. (33) (solid black line) and from analytical relations given by Eqs. (12) (dashed gray line) are compared in Fig. 1. The planet was initially located on the positive x -axis. Initial semimajor axis of the dust particle is (in general) computed from the relation $a_{\text{in}} = a_{n_{\text{P}}/n} + \Delta$, where $a_{n_{\text{P}}/n} = a_{\text{P}} (1 - \beta)^{1/3} (n_{\text{P}}/n)^{2/3}$ (with β calculated from Eq. 3) and Δ is a shift from the exact resonant semimajor axis. As the initial conditions for a dust particle with $R = 2 \mu\text{m}$, mass density $\varrho = 1 \text{ g/cm}^3$, and $\bar{Q}'_{\text{pr}} = 1$, we used $a_{\text{in}} = a_{2/1} + 0.001 \text{ AU}$, $e_{\text{in}} = 0.2$, $\tilde{\omega}_{\text{in}} = 285^\circ$. The initial true anomaly of the dust particle was $f_{\text{in}} = 0$. On the right-hand sides of Eqs. (12) we used numerically calculated values k , h , L , a , e and $\tilde{\omega}$ averaged over the synodic period. Over the synodic period averaged terms $\partial R/\partial a$, $\partial R/\partial e$ and $\partial R/\partial \tilde{\omega}$ were calculated from their definition given by Eq. (8). $\partial R/\partial k$ and $\partial R/\partial h$ in Eqs. (12) were calculated from Eqs. (14) using $\partial R/\partial e$ and $\partial R/\partial \sigma_0$. As can be seen in Fig. 1 numerical and analytical results are in excellent agreement.

8. Types of orbits

The evolution in kh plane is found to be an ideal tool for determining types of orbits. Main property of this plane is its division into sets by a line on which collisions of the planet and the particle take place. The collisions line, for the exterior mean motion orbital 2/1 resonance, is depicted in Figs. 2, 3 and 4 using the dashed line. For this resonance is the phase space practically divided into two sets. Evolutions in the first set are depicted in Figs. 2 and 4. One evolution from the second set is shown in Fig. 3. We used the same parameters to describe the dust particle and the non-gravitational effects as in Sec. 7. We must note that the evolution duration 11.3×10^6 years requires the size of an interstellar gas cloud 303.9 pc in the direction of the interstellar gas velocity vector (constant velocity with magnitude 26.3 km s^{-1} is assumed) and such situation cannot always occur in the real Galactic environment. Evolutions with a such long capture times should be used only for theoretical purposes only. A shorter part of the evolution is still valid. The planet was initially located on the positive x -axis. The initial conditions of the dust particle are in Tab. 1. Orbital evolutions in the second set are characterized by a fast monotonic shift of pericentre and oscillations of eccentricity (Fig. 3). The evolutions in the second set correspond to libration around one of libration centers of conservative problem which is located on the right side from the origin on the h -axis. Orbital evolutions in the first set can be divided into two groups corresponding to two

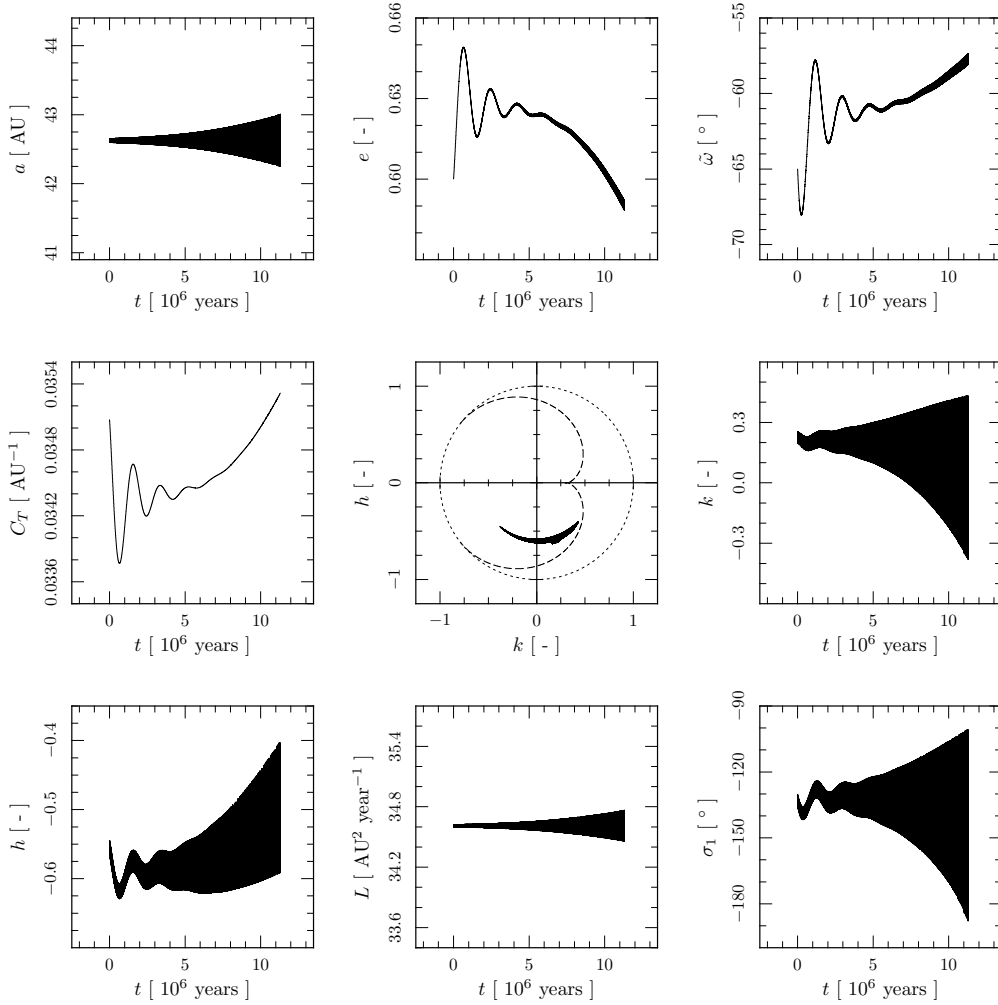


Fig. 2.— From left to right and from top to bottom evolutions of a (semimajor axis), e (eccentricity), $\tilde{\omega}$ (longitude of perihelion), $C_T = (1 - \beta)/(2a) + \sqrt{(1 - \beta)a(1 - e^2)}/a_p^3$ (Tisserand parameter), kh point, $k = e \cos \sigma_0$, $h = e \sin \sigma_0$, $L = \sqrt{\mu(1 - \beta)a}$ and $\sigma_1 = (p + q)\lambda_P/q - p\lambda/q$ for a dust particle with $R = 2 \mu\text{m}$, $\varrho = 1 \text{ g/cm}^3$, and $\bar{Q}'_{\text{pr}} = 1$ captured in an exterior mean motion orbital 2/1 resonance with Neptune under the action of the PR effect, radial solar wind and IGF. In the kh plane resonant libration occurs around the bottom libration center of the conservative problem. Evolutions of the eccentricity and the longitude of perihelion during libration around this center are characterized by damped oscillations approaching to some relatively slowly changing values. The dashed line in the kh plane corresponds to values of e and σ_0 which lead to collisions of the planet and the particle. All parameters are averaged over the synodic period.

libration centers of conservative problem. One evolution with libration around center located below the h -axis (bottom center) is depicted in Fig. 2 and one evolution with libration around center

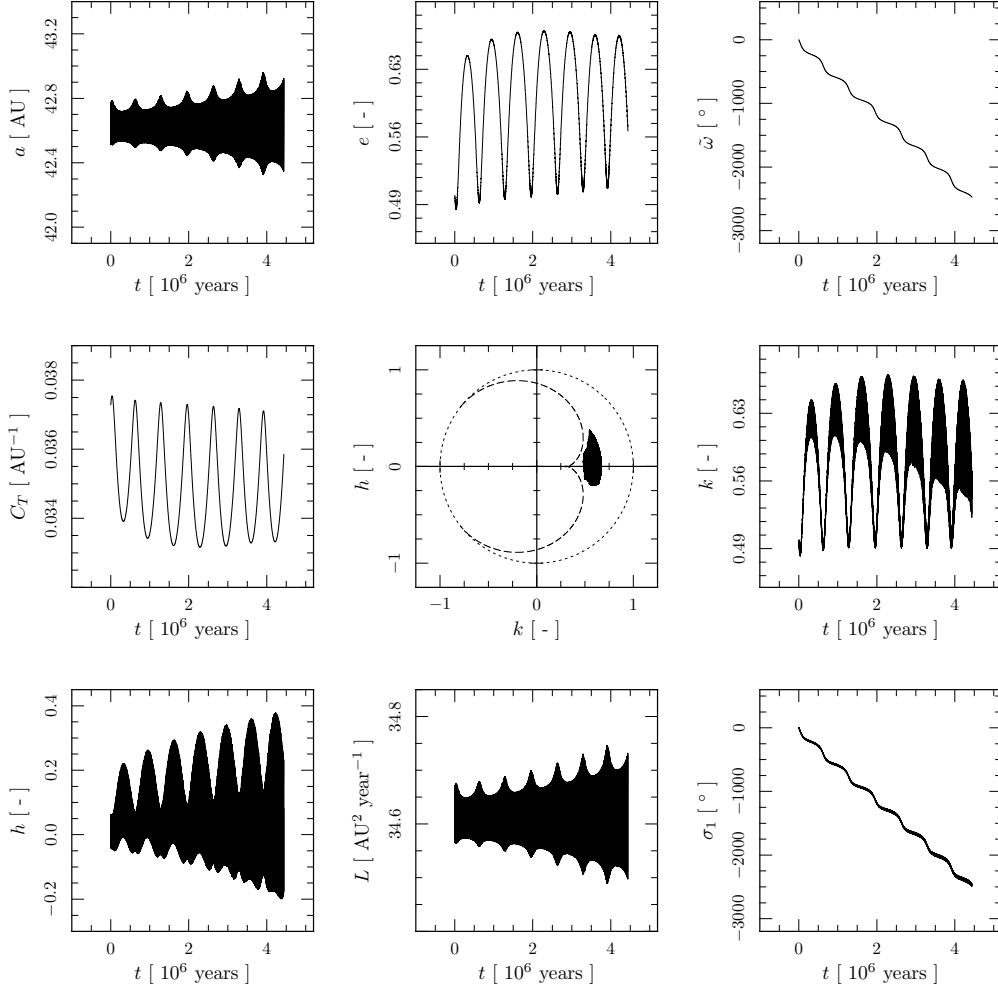


Fig. 3.— Same situation as in Fig. 2, except for resonance with libration around libration center of the conservative problem which is located on the right side from the origin in the kh plane. Orbital evolutions with libration around this center are characterized by oscillations in the eccentricity and a fast monotonic shift of the longitude of perihelion.

located above the h -axis (top center) in Fig. 4. Evolutions of the eccentricity and the longitude of pericentre during libration around the bottom centre are characterized by damped oscillations approaching to some “constant” values. We found that these values are not exactly constant but in comparison with the evolution before this “stabilization” are relatively slowly changing (as can be seen in Fig. 2). Orbital evolutions with libration around the bottom center have larger maximal capture times than evolutions with libration around the top center. The two groups with the largest maximal capture times (the second set and the libration around the bottom center) were already identified in Pástor (2013). For the planet initially located on the positive x -axis and the particle with initial conditions $a_{\text{in}} = a_{2/1}$, e_{in} arbitrary, $\tilde{\omega}_{\text{in}}$ arbitrary and $f_{\text{in}} = 0$ we obtain in

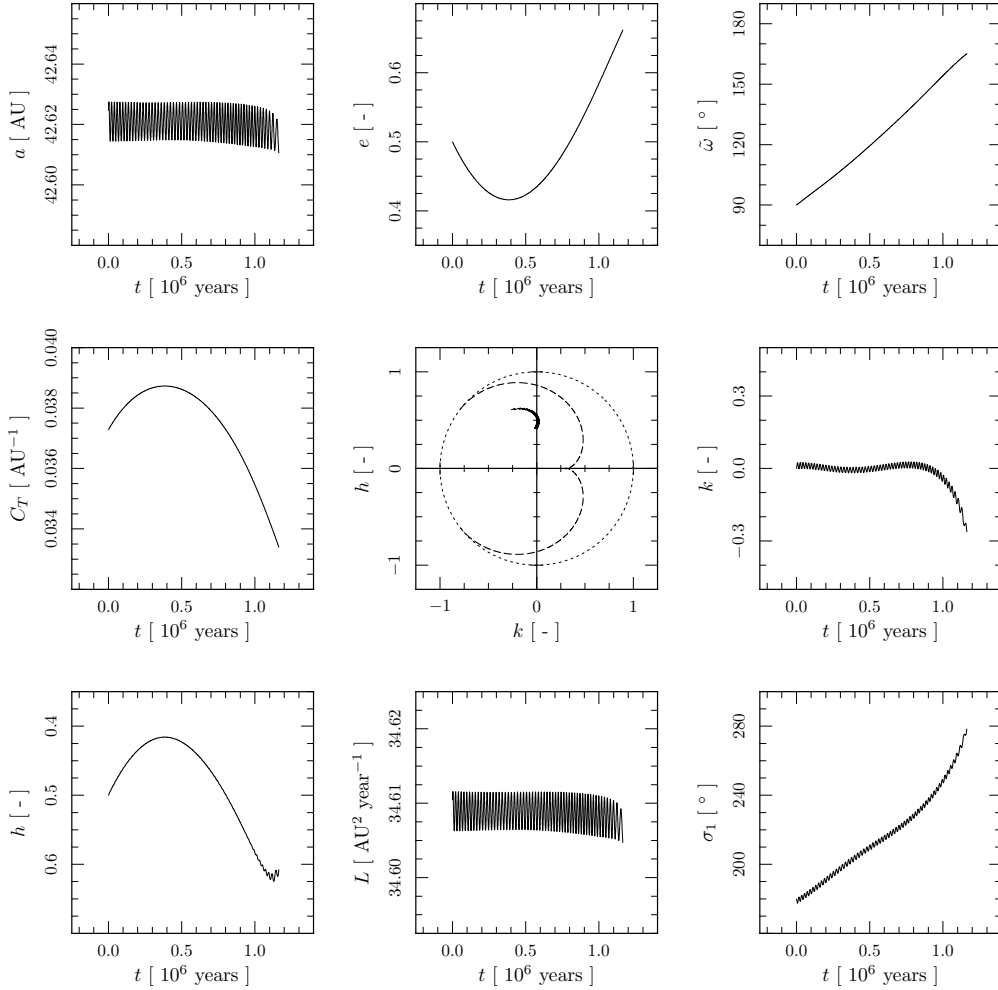


Fig. 4.— Same situation as in Fig. 2, except for resonance with libration around the top libration center of the conservative problem in the kh plane. Maximal capture times of resonances with libration around the top libration center are shorter than maximal capture times of resonances with libration around the bottom and the right libration centers.

$\tilde{\omega}_{in}e_{in}$ plane the collisions line depicted in Fig. 5. This curve divided evolutions in Pástor (2013) into two groups (in our notation the first set and the second set). We found that a horseshoe-like libration between the top and the bottom libration centers in the first set is also possible with smaller maximal capture times.

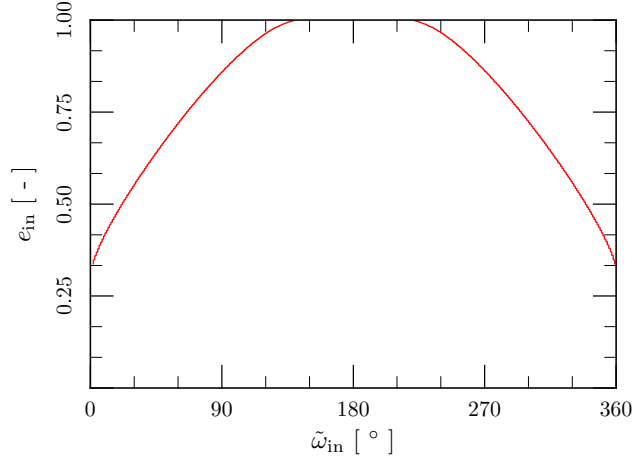


Fig. 5.— In the case when a planet in a circular orbit is initially located on the positive x -axis and a dust particle with $R = 2 \mu\text{m}$, $\rho = 1 \text{ g/cm}^3$, and $\bar{Q}'_{\text{pr}} = 1$ is initially in the perihelion, the depicted curve corresponds to initial longitudes of perihelion and eccentricities of the particle leading to collisions of the planet and the particle for the exact exterior mean motion orbital 2/1 resonance.

9. Searching for stable orbits

Orbital evolutions corresponding to the libration around bottom libration center (Fig. 2) motivated us to search for stable orbits of a dust particle captured in an MMR with a planet under the action of the PR effect, radial stellar wind and IGF. Eqs. (12) enable searching for stable orbits determined by equations

$$\frac{dk}{dt} = \frac{dh}{dt} = \frac{dL}{dt} = 0 . \quad (40)$$

Substitution of Eqs. (40) in Eqs. (12) leads to the conditions

$$\begin{aligned} \langle P_1 \rangle - s \langle P_2 \rangle &= 0 , \\ e \frac{\partial R}{\partial e} &= k \frac{\partial R}{\partial k} + h \frac{\partial R}{\partial h} = \frac{Le^2}{\alpha} \left(\frac{d\sigma_1}{dt} + \langle Q_2 \rangle \right) , \\ \frac{\partial R}{\partial \sigma_0} &= k \frac{\partial R}{\partial h} - h \frac{\partial R}{\partial k} = \langle P_2 \rangle . \end{aligned} \quad (41)$$

The first equation in Eqs. (41) is equivalent with the condition $\langle de/dt \rangle = 0$ (Eq. 20). Eqs. (41) describe also stable orbits with $d\sigma_1/dt \neq 0$, in general. Now we show that such stable orbits are not possible under the action of the considered non-gravitational effects. The second equation of Eqs. (41) can be rewritten using the second equation of Eqs. (15) and the last equation of Eqs. (13) into the following form

$$e \frac{\partial R}{\partial e} = \frac{Le^2}{\alpha} \left(\frac{d\sigma_1}{dt} - \frac{d\tilde{\omega}}{dt} + \frac{\alpha}{Le} \frac{\partial R}{\partial e} \right) . \quad (42)$$

This equation is equivalent with the condition

$$\frac{d\sigma_0}{dt} = \frac{d\sigma_1}{dt} - \frac{d\tilde{\omega}}{dt} = 0 . \quad (43)$$

Therefore, if should be $d\sigma_1/dt \neq 0$, then the longitude of pericentre of the particle orbit must change. Since the eccentricity is a constant for a stable orbit, we can write for the first of Eqs. (41) (see Eqs. 35)

$$B(\tilde{\omega}) = \langle P_1 \rangle - s \langle P_2 \rangle = \alpha_1 S^2 + \alpha_2 I^2 + \alpha_3 I + \alpha_4 = 0 , \quad (44)$$

where α_p for $p = 1, \dots, 4$ are some constants. $B(\tilde{\omega})$ is constant for all $\tilde{\omega}$ and its derivative with respect to the time must be zero. We get

$$\frac{dB}{dt} = \frac{dB}{d\tilde{\omega}} \frac{d\tilde{\omega}}{dt} = (2\alpha_1 I - 2\alpha_2 I - \alpha_3) S \frac{d\tilde{\omega}}{dt} = 0 . \quad (45)$$

Because $\alpha_1 \neq \alpha_2$ and $\alpha_3 \neq 0$, for all existing stable orbits must be

$$\frac{d\tilde{\omega}}{dt} = \frac{d\sigma_1}{dt} = 0 . \quad (46)$$

We come to conclusion that the longitude of pericentre must be constant for all stable orbits. If we use Eq. (40) and Eq. (46) in Eqs. (12), we obtain for the considered non-gravitational effects the following conditions for searching of the stable orbits

$$\begin{aligned} \langle P_1 \rangle - s \langle P_2 \rangle &= 0 , \\ \frac{\partial R}{\partial e} &= \frac{Le}{\alpha} \langle Q_2 \rangle , \\ \frac{\partial R}{\partial \sigma_0} &= \langle P_2 \rangle , \\ \frac{2sL}{\mu(1-\beta)} \frac{\partial R}{\partial a} &= -n_P \frac{p+q}{q} + ns - s \langle Q_1 \rangle + (1-\alpha) s \langle Q_2 \rangle . \end{aligned} \quad (47)$$

9.1. Application on the exterior mean motion orbital 2/1 resonance with Neptune

We have searched stable orbits for a particle captured in the exterior mean motion orbital 2/1 resonance with Neptune under the action of PR effect, radial solar wind and IGF. The particle and the non-gravitational effects were described by the same parameters as in Sec. 7. The relation depicted in Fig. 6 represents couplets of $\tilde{\omega}$ and e for which the first equation of Eqs. (47) holds. Any stable solution must lie on this curve. Also the secular time derivative of eccentricity averaged over a libration period is zero for the points on the curve (Appendix 3). Solutions of three remaining equations in the system of equations given by Eqs. (47) represent points in four dimensional space with e_{in} , $\tilde{\omega}_{\text{in}}$, f_{in} and $f_{\text{P in}}$ on axes. Here, f_{in} and $f_{\text{P in}}$ are initial true anomalies of the particle and the planet, respectively. If we consider an exact resonance with $n_P(p+q) = np$, then further

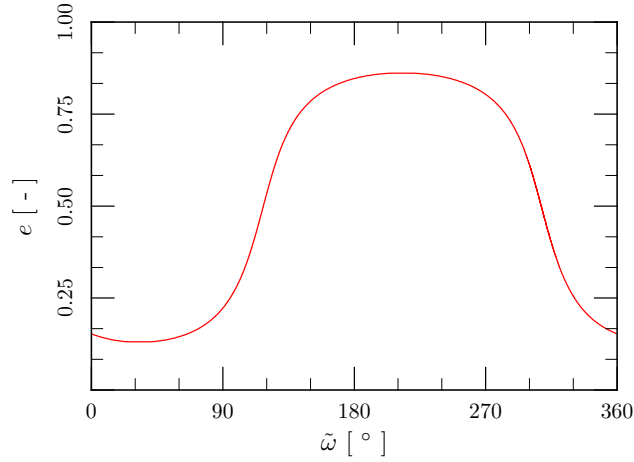


Fig. 6.— Couples of the longitude of perihelion and the eccentricity for which the first equation of system Eqs. 47 hold for a dust particle with $R = 2 \mu\text{m}$, $\rho = 1 \text{ g/cm}^3$, and $\bar{Q}'_{\text{pr}} = 1$ captured in an exterior mean motion orbital 2/1 resonance with Neptune under the action of the PR effect, radial solar wind and IGF.

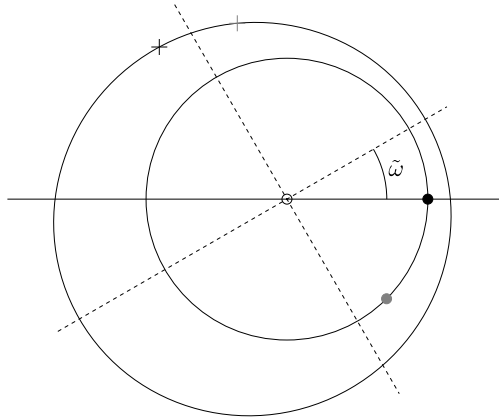


Fig. 7.— A dust particle captured in an exact exterior mean motion orbital 2/1 resonance with a planet. Positions of the planet and the dust particle in two different times are depicted with different colors. If are these positions used as initial positions for averaging of terms $\partial R/\partial e$, $\partial R/\partial \sigma_0$ and $\partial R/\partial a$ over the synodic period ($2\pi p/n_P$ for the exact resonance), obtained result are the same in both cases.

reduction of the dimension number is possible. Due to the exact resonance for all initial positions of the planet and all initial positions of the dust particle, we can find the same value of over the synodic period averaged terms $\partial R/\partial e$, $\partial R/\partial \sigma_0$ and $\partial R/\partial a$ for a fixed initial position of the planet and calculated initial positions of the dust particle. Two such equivalent initial positions of the

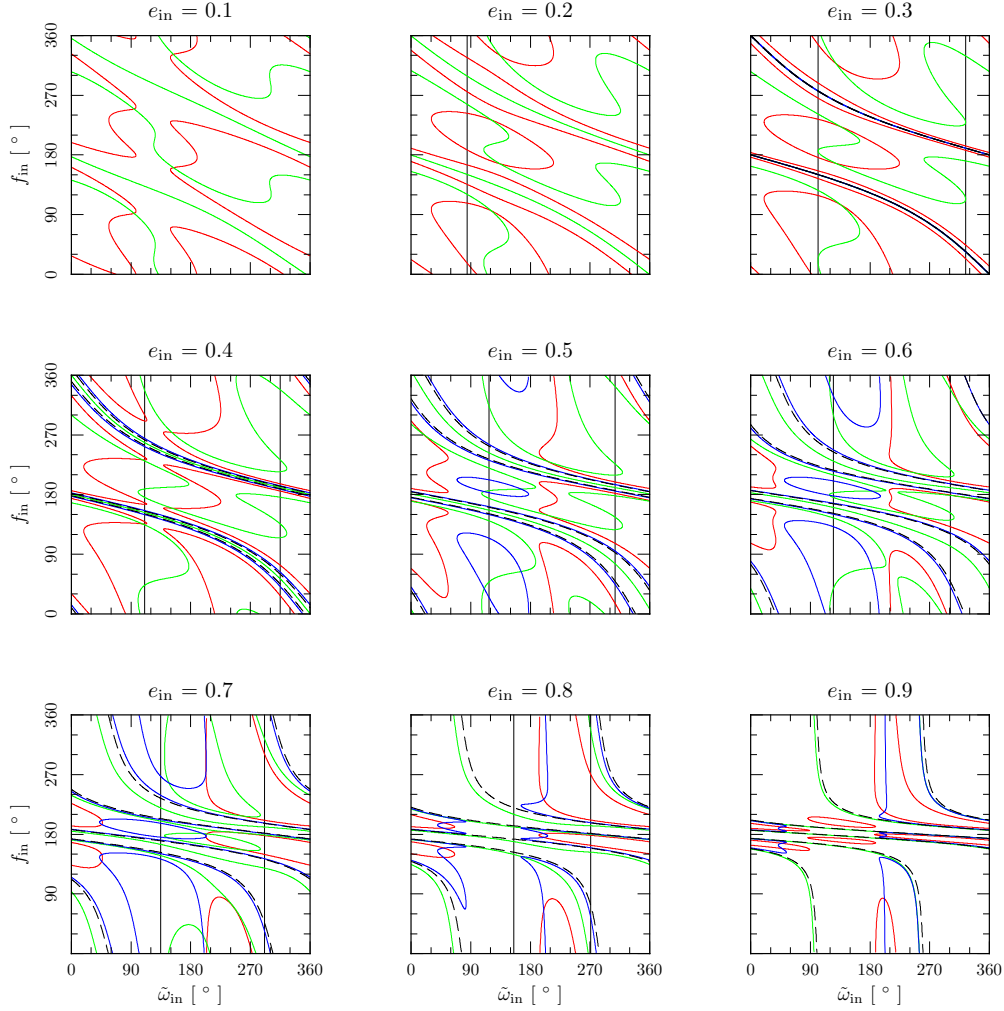


Fig. 8.— Sections of three dimensional phase space determined by solutions of last three equations in Eqs. (47) for a dust particle with $R = 2 \mu\text{m}$, $\rho = 1 \text{ g/cm}^3$, and $\bar{Q}'_{\text{pr}} = 1$ captured in the exact exterior mean motion orbital 2/1 resonance with Neptune under the action of the PR effect, radial solar wind and IGF. Vertical lines in a given section correspond to the longitude of perihelion for which the first equation of Eqs. (47) hold. Lines with red, green and blue color correspond to solutions of the second, third and fourth equation in Eqs. (47), respectively. Collisions of the planet with the particle occur for points on the dashed lines.

planet and the dust particle are depicted in Fig. 7. The fixed initial position of the planet is on the horizontal axis depicted with the black circle. The chosen initial positions of the planet and the dust particle are depicted with a gray color. The calculated initial position of the dust particle corresponds to the position of the dust particle after the time during which the planet moves into the fixed initial position. This couple of initial positions have the same value of over the synodic

period averaged terms $\partial R/\partial e$, $\partial R/\partial \sigma_0$ and $\partial R/\partial a$. Hence, solutions of last three equations in the system of equations given by Eqs. (47) for the exact resonance represent points in three dimensional space with e_{in} , $\tilde{\omega}_{\text{in}}$, f_{in} on axes. Sections of this phase space are shown for nine different initial eccentricities in Fig. 8. The fixed initial position of the planet was on the positive x -axis. Points with red, green and blue color correspond to solutions of the second, third and fourth equation in Eqs. (47), respectively. Points on dashed lines in Fig. 8 lead to collisions of the planet with the particle. The perihelion distance is larger than the radius of planet's orbit for $e_{\text{in}} \lesssim 0.2945$. Therefore, dashed lines are not on the sections with initial eccentricity equal to 0.1 and 0.2. Since the planet initial position is fixed, for every orbit with $e_{\text{in}} \gtrsim 0.2945$ exists some true anomalies of the particle which lead to the collisions. Vertical lines in a given section are on positions given by the longitudes of perihelion for which the first equation of Eqs. (47) hold (see also Fig. 6). Fig. 8 allows to determine the stable orbits in the exact resonance under the action of the PR effect, radial stellar wind and IGF. As can be seen in Fig. 8 there is no a common point for the red, green, blue and vertical line. Therefore, any stable solution in Fig. 8 does not exist. We have not found any stable solution also for sections with greater resolution in the initial eccentricity. The evolution shown in Fig. 2 clearly does not represent a stable solution determined by Eqs. (47) because parameters k and h rapidly change during the evolution.

10. Conclusion

From a near canonical form of equations of motion in cartesian coordinates we derived averaged resonant equations for a circumstellar dust particle captured in an MMR with a planet in a circular orbit under the action of given non-gravitational effects in general form. The averaged resonant equations were also obtained/confirmed using the Lagrange's planetary equations. We considered also non-gravitational effects for which secular variations of the orbit depend on the orientation of orbit in space. This access enabled us to investigate the motion of dust particle in an MMR under the action of the PR effect, radial stellar wind and interstellar wind. Comparison of analytically and numerically calculated averaged time derivatives of non-canonical resonant variables showed excellent agreement. From numerical solutions of equation of motion evolutions in kh plane can be obtained. Using evolutions in the kh plane types of orbits can be easily determined. We found that for the exterior mean motion orbital 2/1 resonance all types of orbits correspond to libration centers of conservative problem. The averaged resonant equations enable finding of stationary solutions for the particle orbit. We analytically showed that any stationary solution with the shift of pericentre can not exist. Using a numerical solution of equations obtained from the averaged resonant equations we showed that also any stationary solution without the shift of pericentre can not exist.

REFERENCES

- Alouani-Bibi F., Opher M., Alexashov D., Izmodenov V., Toth G., 2011. Kinetic versus multi-fluid approach for interstellar neutrals in the heliosphere: exploration of the interstellar magnetic field effects. *Astrophys. J.* **734**, 45.
- Baines M. J., Williams I. P., Asebiomo A. S., 1965. Resistance to the motion of a small sphere moving through a gas. *Mon. Not. R. Astron. Soc.* **130**, 63-74.
- Belyaev M., Rafikov R., 2010. The dynamics of dust grains in the outer Solar system. *Astrophys. J.* **723**, 1718-1735.
- Bate R. R., Mueller D. D., White J. E., 1971. *Fundamentals of Astrodynamics* Dover Publications, New York
- Beaugé C., Ferraz-Mello S., 1993. Resonance trapping in the primordial solar nebula: the case of a Stokes drag dissipation. *Icarus* **103**, 301-318.
- Beaugé C., Ferraz-Mello S., 1994. Capture in exterior mean-motion resonances due to Poynting-Robertson drag. *Icarus* **110**, 239-260.
- Brouwer D., Hori G. I., 1961. Theoretical evaluation of atmospheric drag effects in the motion of an artificial satellite. *Astron. J.* **66**, 193-225.
- Brownlee D. E., 1994. The ring around us. *Nature* **369**, 706.
- Buenzli E., Thalmann C., Vigan A., Boccaletti A., Chauvin G., Augereau J. C., Meyer M. R., Mnard F., Desidera S., Messina S., Henning T., Carson J., Montagnier G., Beuzit J. L., Bonavita M., Eggenberger A., Lagrange A. M., Mesa D., Mouillet D., Quanz S. P., 2010. Dissecting the Moth: discovery of an off-centered ring in the HD 61005 debris disk with high-resolution imaging. *Astron. Astrophys.* **524**, L1.
- Danby J. M. A., 1988. *Fundamentals of Celestial Mechanics* 2nd edn., Willmann-Bell, Richmond.
- Debes J. H., Weinberger A. J., Kuchner M. J., 2009. Interstellar medium sculpting of the HD 32297 debris disk. *Astrophys. J.* **702**, 318-326.
- Dermott S. F., Jayaraman S., Xu Y. L., Gustafson B. A. S., Liou J. C., 1994. A circumsolar ring of asteroidal dust in resonant lock with the Earth. *Nature* **369**, 719-723.
- Dermott S. F., Grogan K., Durda D. D., Jayaraman S., Kehoe T. J. J., Kortenkamp S. J., Wyatt M. C., 2001. Orbital evolution of interplanetary dust. In: Grün E., Gustafson B. A. S., Dermott S. F., Fechtig H. (eds.), *Interplanetary Dust*, Springer-Verlag, Berlin, pp. 569-639.
- Dohnanyi J. S., 1978. Particle dynamics. In: McDonnell J. A. M. (ed.), *Cosmic Dust*, Wiley-Interscience, Chichester, pp. 527-605.

- Frisch P. C., Bzowski M., Grün E., Izmodenov V., Krüger H., Linsky J. L., McComas D. J., Möbius E., Redfield S., Schwadron N., Shelton R., Slavin J. D., Wood B. E., 2009. The galactic environment of the Sun: interstellar material inside and outside of the heliosphere. *Space Sci. Rev.* **146**, 235-273.
- Golimowski D. A., Krist J. E., Stapelfeldt K. R., Chen C. H., Ardila D. R., Bryden G., Clampin M., Ford H. C., Illingworth G. D., Plavchan P., Rieke G. H., Su K. Y. L., 2011. Hubble and Spitzer Space Telescope observations of the debris disk around the nearby K dwarf HD 92945. *Astrophys. J.* **142**, 30.
- Gustafson B. A. S., 1994. Physics of zodiacal dust. *Annu. Rev. Earth Planet. Sci.* **22**, 553-595.
- Hines D. C., Schneider G., Hollenbach D., Mamajek E. E., Hillenbrand L. A., Metchev S. A., Meyer M. R., Carpenter J. M., Moro-Martín A., Silverstone M. D., Kim J. S., Henning T., Bouwman J., Wolf S., 2007. The Moth: an unusual circumstellar structure associated with HD 61005. *Astrophys. J.* **671**, L165-L168.
- Kirkwood D., 1867. *Meteoric Astronomy: A Treatise on Shooting-Stars, Fireballs, and Aerolites* Lippincott J. B. & co., Philadelphia.
- Klačka J., 2008. Electromagnetic radiation, motion of a particle and energy-mass relation. arXiv: 0807.2915.
- Klačka J., Kómar L., Pástor P., Petržala J., 2008. The non-radial component of the solar wind and motion of dust near mean motion resonances with planets. *Astron. Astrophys.* **489**, 787-793.
- Klačka J., Petržala J., Pástor P., Kómar L., 2012. Solar wind and motion of dust grains. *Mon. Not. R. Astron. Soc.* **421**, 943-959.
- Klačka J., Petržala J., Pástor P., Kómar L., 2013. The Poynting-Robertson effect: a critical perspective. *Icarus* in press, doi:10.1016/j.icarus.2012.06.044
- Lallement R., Quémerais E., Bertaux J.L., Ferron S., Koutroumpa D., Pellinen R., 2005. Deflection of the interstellar neutral hydrogen flow across the heliospheric interface. *Science* **307**, 14471449.
- Leinert C., Grün E., 1990. Interplanetary dust. In: Schwen R., Marsch E. (eds.), *Physics of the Inner Heliosphere I*, Springer-Verlag, Berlin, pp. 207-275.
- Liou J.-Ch., Zook H. A., 1997. Evolution of interplanetary dust particles in mean motion resonances with planets. *Icarus* **128**, 354-367.
- Maness H. L., Kalas P., Peek K. M. G., Chiang E. I., Scherer K., Fitzgerald M. P., Graham J. R., Hines D. C., Schneider G., Metchev S. A., 2009. Hubble Space Telescope optical imaging of the eroding debris disk HD 61005. *Astrophys. J.* **707**, 1098-1114.

- Marzari F., 2012. Interstellar medium perturbations on transport-dominated debris discs in binary star systems. *Mon. Not. R. Astron. Soc.* **421**, 3431-3442.
- Marzari F., Thébault P., 2011. On how optical depth tunes the effects of the interstellar medium on debris discs. *Mon. Not. R. Astron. Soc.* **416**, 1890-1899.
- Murray C. D., Dermott S. F., 1999. *Solar System Dynamics* Cambridge University Press, New York.
- Pástor P., 2012a. Influence of fast interstellar gas flow on the dynamics of dust grains. *Celest. Mech. Dyn. Astron.* **112**, 23-45.
- Pástor P., 2012b. Orbital evolution under the action of fast interstellar gas flow with a non-constant drag coefficient. *Mon. Not. R. Astron. Soc.* **426**, 1050-1060.
- Pástor P., 2013. Dust particles in mean motion resonances influenced by an interstellar gas flow. *Mon. Not. R. Astron. Soc.* **431**, 3139-3149.
- Pástor P., Klačka J., Kómar L., 2009. Motion of dust in mean motion resonances with planets. *Celest. Mech. Dyn. Astron.* **103**, 343-364.
- Pástor P., Klačka J., Kómar L., 2011. Orbital evolution under the action of fast interstellar gas flow. *Mon. Not. R. Astron. Soc.* **415**, 2637-2651.
- Pástor P., Klačka J., Petržala J., Kómar L., 2009. Eccentricity evolution in mean motion resonance and non-radial solar wind. *Astron. Astrophys.* **501**, 367-374.
- Poynting J. M., 1904. Radiation in the Solar system: its effect on temperature and its pressure on small bodies. *Philos. Trans. R. Soc. Lond. Ser. A* **202**, 525-552.
- Reach W. T., Franz B. A., Welland J. L., Hauser M. G., Kelsall T. N., Wright E. L., Rawley G., Stemwedel S. W., Spleman W. J., 1995. Observational confirmation of a circumsolar dust ring by the COBE satellite. *Nature* **374**, 521-523.
- Robertson H. P., 1937. Dynamical effects of radiation in the Solar system. *Mon. Not. R. Astron. Soc.* **97**, 423-438.
- Rodigas T. J., Hinz P. M., Leisenring J., Vaitheeswaran V., Skemer A. J., Skrutskie M., Su K. Y. L., Bailey V., Schneider G., Close L., Mannucci F., Esposito S., Arcidiacono C., Pinna E., Argomedo J., Agapito G., Apai D., Bono G., Boutsia K., Briguglio R., Brusa G., Busoni L., Cresci G., Currie T., Desidera S., Eisner J., Falomo R., Fini L., Follette K., Fontana A., Garnavich P., Gratton R., Green R., Guerra J. C., Hill J. M., Hoffmann W. F., Jones T. J., Krejny M., Kulesa C., Males J., Masciadri E., Mesa D., McCarthy D., Meyer M., Miller D., Nelson M. J., Puglisi A., Quiros-Pacheco F., Riccardi A., Sani E., Stefanini P., Testa V., Wilson J., Woodward C. E., Xompero M., 2012. The gray needle: large grains in the HD

15115 debris disk from LBT/PISCES/ K_s and LBTI/LMIRcam/ L' adaptive optics imaging. *Astrophys. J.* **752**, 57.

Whipple F. L., 1955. A comet model III. The zodiacal light. *Astrophys. J.* **121**, 750-770.